Resonances in the K shell excitation spectra of benzene and pyridine: Gas phase, solid, and chemisorbed states

J. A. Horsley and J. Stöhr[a)]
Corporate Research Science Laboratories, Exxon Research and Engineering Company, Annandale, New Jersey 08801

A. P. Hitchcock and D. C. Newbury
Department of Chemistry, McMaster University, Hamilton, Canada L8S 4M1

A. L. Johnson
Department of Chemistry, University of California, Berkeley, California 94720

F. Sette
AT&T Bell Laboratories, Murray Hill, New Jersey 07974

(Received 14 June 1985; accepted 3 September 1985)

K shell excitation spectra of the aromatic molecules benzene and pyridine in the gas phase are compared to those for the solids (ices) and for monolayers chemisorbed on Pt(111). The gas phase and solid spectra are essentially identical and even the spectra for the chemisorbed molecules exhibit the same resonances. Because of the orientation of the molecules upon chemisorption the latter spectra show a strong polarization dependence as a function of x-ray incidence. This polarization dependence in conjunction with a multiple scattering $X\alpha$ calculation for the benzene molecule allows us to assign the origin of all K shell resonances. The resonances are found to arise from transitions to π^* antibonding orbitals and to σ^* shape resonances in the continuum. The shape resonances are characterized by potential barriers in high ($l = 5$ and 6) angular momentum states of the excited photoelectron. The polarization dependence and energy position of the resonances allow the molecular orientation on the surface to be determined and show that the change in the carbon–carbon bond length is less than 0.02 Å.

I. INTRODUCTION

Inner shell excitation spectroscopy is proving to be a powerful technique for obtaining information on the electronic structure and geometry of molecules, both in the gas phase[1–3] and adsorbed on surfaces.[4] Inner shell electron energy loss (ISEELS) measurements of K shell resonances in small molecules have recently been combined with soft x-ray absorption measurements of the corresponding resonances in chemisorbed molecules to obtain bond lengths in the adsorbed species to an accuracy of 0.04 Å.[5,6] The molecules studied were fairly simple hydrocarbons and oxygenated species, where the assignment of the K shell resonance is fairly straightforward. Recently, K shell spectra of more complex, aromatic species have been obtained and used to study the surface chemistry of *aromatic* molecules.[7] However, uncertainties in the assignment of the observed resonances have prevented the extension of the approach used to obtain geometrical information on the simpler hydrocarbons to these more complex molecules. We present here the first assignment of all the near edge resonances in the K shell excitation spectra of the benzene and pyridine molecules. This assignment is based in part on a multiple scattering calculation for benzene that accurately reproduces the relative positions and intensities of the observed resonances. By comparing the observed resonances for the gas phase molecule with the corresponding resonances for benzene and pyridine chemisorbed on Pt(111) we obtain information on the orientation and geometry of the adsorbed species. In contrast to the simpler unsaturated hydrocarbons studied previously,[6] we find no measurable change in molecular geometry on chemisorption.

II. EXPERIMENTAL DETAILS

Gas phase K shell excitation spectra were recorded by inner shell electron energy loss spectroscopy (ISEELS) which, in the limit of small momentum transfer, yields results which are equivalent to x-ray absorption spectroscopy. The basic apparatus and experimental technique have been described previously.[2] Recently the apparatus has been modified to differentially pump the electron gun in order to improve spectrometer stability by reducing the interaction of chemically active gases with the electron emitting surface. Briefly, the benzene and pyridine spectra were obtained by measurement of the energy loss signal at small scattering angle (2×10^{-2} rad) of 2.8 keV incident electrons. The carbon K shell spectrum of gaseous benzene was essentially identical to that obtained from earlier ISEELS studies under similar experimental conditions.[8] The K shell spectra of gaseous pyridine have not been reported previously to our knowledge. The absolute energy scales at the C and N K edges of the gas phase spectra were calibrated (accurate to $\pm$ 0.1 eV) with respect to the C and N ($1s \rightarrow \pi^*$) excitations in the gas phase spectra of CO and N_2. The samples were obtained from the vapor of high purity liquids. In order to eliminate air and other volatile impurities the liquids were subjected to several freeze–pump–thaw cycles.

Near edge x-ray absorption fine structure (NEXAFS)

[a)] Present address: IBM, San Jose Research Laboratory, 5600 Cottle Rd., San Jose, California 95193.

 © 1985 American Institute of Physics

Downloaded 18 Jun 2002 to 130.113.69.66. Redistribution subject to AIP license or copyright, see http://ojps.aip.org/jcpo/jcpcr.jsp

spectra of condensed multilayers and chemisorbed monolayers were recorded with soft x rays using the grasshopper monochromator on beam line I-1 at the Stanford Synchrotron Radiation Laboratory. The *K* shell absorption was monitored by means of partial electron yield detection. The electron detector consisted of two high transmission metal grids and a dual channel plate array. The first grid was kept at ground potential while retarding voltages of -200 and -320 eV were applied to the second grid for the C and N *K* edge spectra, respectively. The x-ray incidence angle on the sample could be varied from grazing incidence ($\theta = 20°$), with the electric field vector E close to the surface normal, to normal incidence ($\theta = 90°$), with E parallel to the surface. The photon energy transmitted by the monochromator was calibrated in the carbon 1*s* region to an accuracy of ± 0.5 eV. In the nitrogen 1*s* region the monochromator was not specifically calibrated. In this energy region the absolute energy may be in error by as much as 1 eV.

The Pt(111) crystal was cleaned by exposure to 10^{-7} Torr oxygen at 870 K followed by annealing in ultrahigh vacuum to 1200 K with argon ion sputtering to remove S when required. The base pressure in the sample chamber was 8×10^{-11} Torr. Solids of benzene and pyridine were prepared by dosing the Pt(111) crystal kept at 100 K with 6×10^{-6} Torr s (6 Langmuir or 6 L) of gas. Monolayers of benzene were obtained by annealing to 200 K or by dosing at 300 K. For pyridine monolayers were obtained by dosing the Pt(111) crystal kept at room temperature to saturation (24 L) coverage.

III. EXPERIMENTAL RESULTS

The gas phase *K* shell excitation spectrum of benzene is shown at the top of Fig. 1. At this resolution there are four main resonances, labeled A–D, with additional weak features between A–B and B–C. The principal resonances have the same position and relative intensity in the spectrum of the solid, shown below the gas phase spectrum, which demonstrates that all the resonances are highy localized on the benzene molecule. The near edge resonances at the C *K*edge in the absorption spectrum of benzene on Pt(111) are shown for perpendicular and grazing x-ray incidence in the lower two curves of Fig. 1. As pointed out previously,[7] the polarization dependence of the broad π^* resonance at 285 eV indicates that the benzene molecules lie in a plane parallel to the surface, in agreement with the results of other surface science techniques.[9–11] There are clearly two peaks at higher energy that match up well with the positions of the peaks C and D in the gas phase spectrum. The increased width of the resonances in the monolayer spectra is not of instrumental origin, but occurs because of the interaction of the benzene molecules with the Pt(111) surface, as discussed in a later section. The positions and assignments of the spectral features in all of the benzene spectra are listed in Table I.

In the spectra of Fig. 1 the *K* shell ionization threshold (I.P.) in each phase is indicated by the hatched line and labeled C_K. These values were taken from x-ray photoelectron measurements in the gas phase,[12] solid state,[13] and chemisorbed cases. For the gas phase spectrum the I.P. corresponds to the 1*s* binding energy (BE) relative to the vacuum level (E_v) while for the solid and chemisorbed case it corresponds to the 1*s* BE relative to the Fermi level (E_F). For the gas phase spectrum resonances A and B fall below the I.P. and are therefore bound state transitions. For the neutral molecule the antibonding π^* states into which the 1*s* electron is excited fall just above E_v, but in x-ray absorption they are pulled below E_v by the Coulomb interaction with the 1*s* core hole. For solid benzene, which is an insulator, the Fermi level falls in the band gap and the resonance energies for the $1s \rightarrow \pi^*$ transitions can either be smaller or larger than the 1*s* BE's, as observed for peaks A and B, respectively. For a chemisorbed molecular monolayer on a metal surface the lowest possible 1*s* excitation energy is determined by the 1*s* BE relative to the E_F since by definition all states below E_F are filled. Therefore the $1s \rightarrow \pi^*$ transition energy is slightly larger than the 1*s* BE, in agreement with all previously studied cases.[5,6,14]

The C *K* edge spectra of pyridine in the gas, solid, and monolayer phases are shown as recorded in Fig. 2 while Fig. 3 shows the spectra after subtraction of the estimated backgrounds indicated by the dashed lines in Fig. 2. A similar background subtraction procedure has been applied to the benzene spectra (Fig. 1) and the N *K* edge spectra of pyridine

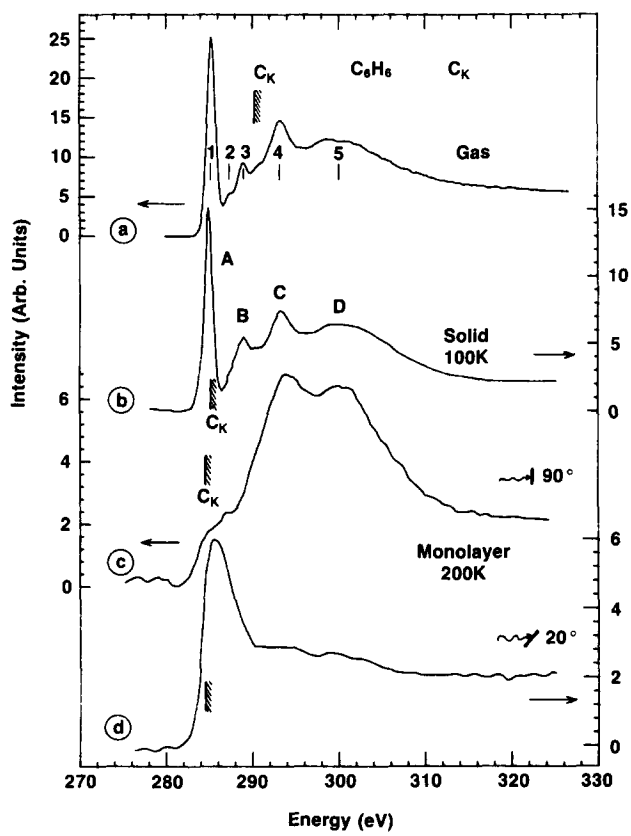

FIG. 1. (a) The carbon *K* shell ISEELS spectrum of gaseous benzene recorded by electron energy loss of 2.8 keV electrons at 1.0 eV FWHM resolution. (b) The carbon *K* shell NEXAFS spectrum of solid benzene recorded by partial electron yield from a multilayer condensate on Pt(111) at 100 K. (c) The partial electron yield NEXAFS spectrum at normal x-ray incidence of monolayer benzene on Pt(111) at 100 K, after heating the sample in (b) to 200 K. (d) The monolayer benzene NEXAFS spectrum recorded at glancing x-ray incidence (20°). A background has been subtracted from each spectrum.

Downloaded 18 Jun 2002 to 130.113.69.66. Redistribution subject to AIP license or copyright, see http://ojps.aip.org/jcpo/jcpcr.jsp

TABLE I. Absolute energies (eV) and assignments of features in the carbon *K* shell spectra of benzene in the gas, solid, and monolayer states.

			Monolayer on Pt(111)		
Feature	Gas ± 0.1 eV	Solid ± 0.5 eV	90° ± 0.5 eV	20° ± 0.5 eV	Assignment[b]
1 (A)	285.2[a]	285.0	...	286.0	$\pi^*(e_{2u})$
2	287.2	...	...	...	$3p$
3 (B)	288.9	288.9	...	...	$\pi_*(b_{2g})$
4 (C)	293.5	293.3	293.7	...	$\sigma^*(e_{1u})$
5 (D)	300.2	300.1	299.9	...	$\sigma^*(e_{2g}^+ a_{2g})$
I.P.	290.3[c]	284.9[d]	284.4[e]	284.4[e]	

[a] ISEELS spectrum recorded with 1.0 eV FWHM. Feature 1 was determined to be 2.2 (1) eV lower in energy than the C $1s \rightarrow \pi^*$ transition in CO [287.40 eV (Ref. 39)].
[b] Only the final orbital is listed.
[c] From gas phase XPS (Ref. 12), relative to vacuum level.
[d] From solid state XPS (Ref. 13), relative to Fermi level.
[e] R. J. Koestner (private communication), relative to Fermi level.

(Fig. 4). The pyridine spectra closely resemble those for benzene. Again the spectra are dominated by four peaks (labeled A–D). At monolayer coverage resonances A and B exhibit the opposite polarization dependence to that of C and D. Also, the dependence on x-ray incidence is reversed from that for benzene. This has been used previously[7] to determine a near-vertical orientation of the ring plane on the Pt(111) surface. The energy position of the I.P.'s relative to the peaks A and B is similar to the situation in benzene. Table II gives the energy positions of all the observed features in the pyridine C *K* edge spectra.

The N *K* edge spectra of gas, solid, and monolayer pyr-

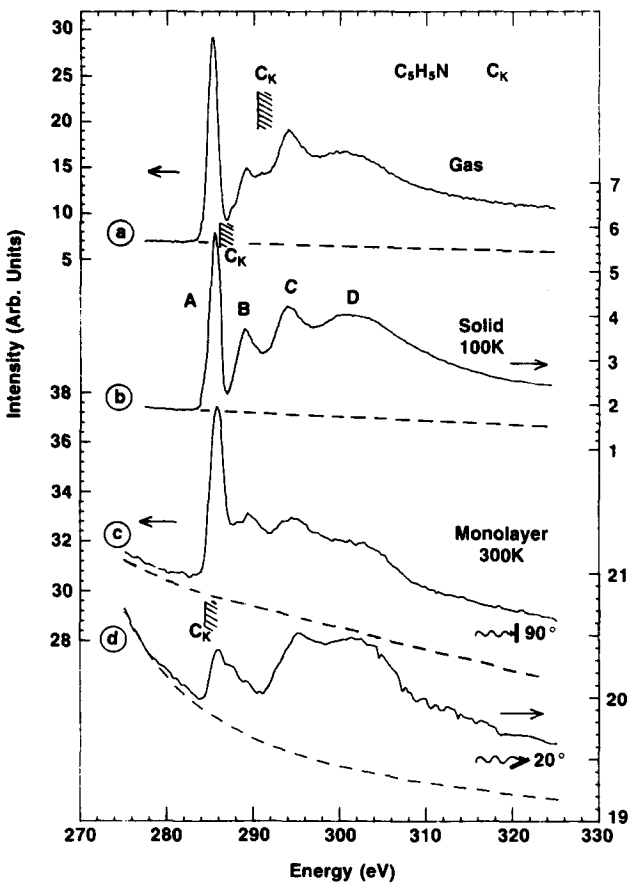

FIG. 2. (a) The carbon *K* shell ISEELS spectrum of gaseous pyridine as recorded. (b) The carbon *K* shell NEXAFS spectrum of solid pyridine as recorded by partial electron yield from a multilayer condensate on Pt(111) at 100 K. (c) The partial electron yield carbon *K* shell NEXAFS spectrum of a monolayer of pyridine on Pt(111) at room temperature as recorded with normal incidence. (d) The monolayer pyridine NEXAFS spectrum as recorded with glancing incidence (20°). In each spectrum the dashed line indicates the estimated instrumental and valence continuum background.

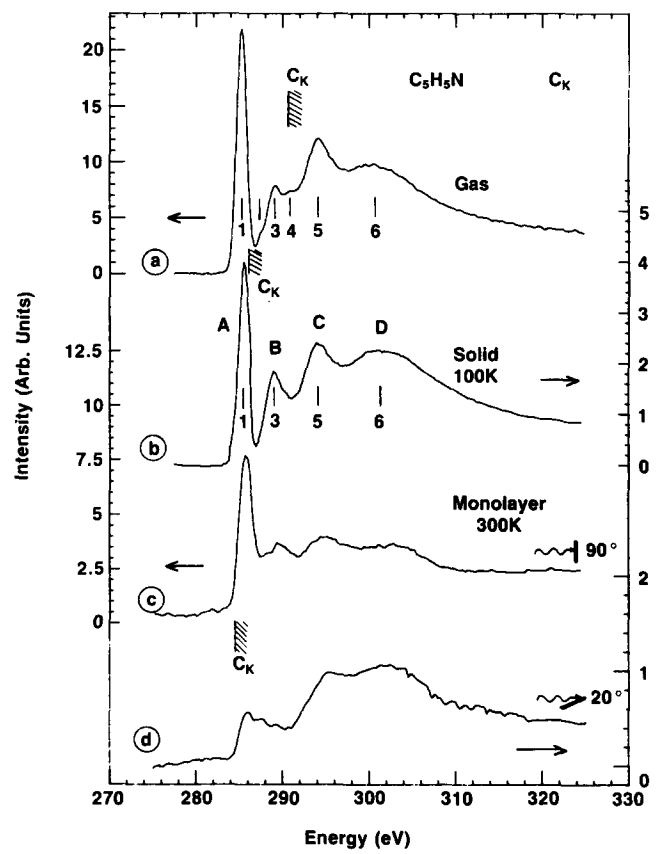

FIG. 3. The background subtracted, pyridine carbon *K* shell spectra of (a) gas, (b) solid, (c) monolayer on Pt(111) at normal incidence, and (d) monolayer on Pt(111) at 20° incidence. These spectra are the difference of the solid and dashed lines in Fig. 2.

Downloaded 18 Jun 2002 to 130.113.69.66. Redistribution subject to AIP license or copyright, see http://ojps.aip.org/jcpo/jcpcr.jsp

TABLE II. Absolute energies (eV) and assignments of features in the carbon *K* shell spectra of pyridine in the gas, solid, and monolayer states.

Feature	Gas ± 0.1 eV	Solid ± 0.5 eV	Monolayer on Pt(111) 90° ± 0.5 eV	Monolayer on Pt(111) 20° ± 0.5 eV	Assignment
1 (A)	285.3[a]	285.5	285.8	285.9	π^*
2	287.4	...	...	...	3*p* Rydberg
3 (B)	289.2	289.1	289.6	...	π^*
4	290.8	...	...	...	continuum onset
5 (C)	294.2	294.1	294.7	295.3	σ^*
6 (D)	300.1	301.0	302.0	301.7	σ^*
I.P.	290.6[b]	285.9[c]	284.4[d]	284.4	

[a] This feature was found to occur at 2.1(1) eV lower in energy than the C $1s \rightarrow \pi^*$ transition in CO [287.40 eV (Ref. 39)].
[b] Obtained from the solid state average carbon 1*s* I.P. (285.9 eV) (Ref. 37) and the differences in gas (Ref. 38) and solid state (Ref. 37) nitrogen 1*s* I.P.'s for pyridine (4.7 eV).
[c] Average of the 3 carbon 1*s* environments (Ref. 37).
[d] Value for benzene on Pt(111).

idine are shown in Fig. 4. In this case only a normal incidence monolayer spectrum was recorded. The pyridine N *K* edge spectra are similar to the corresponding C *K* edge spectra, although the relative intensities of peaks A and B are slightly different, as are the relative intensities of peaks C and D. The position of the N *K* I.P. relative to the peaks in the three phases parallels that in the C *K* edge spectra. The shoulder on the low energy side of the first N *K* edge peak (A) in the solid and monolayer spectra is an instrumental artifact from a non-Gaussian monochromator response function.

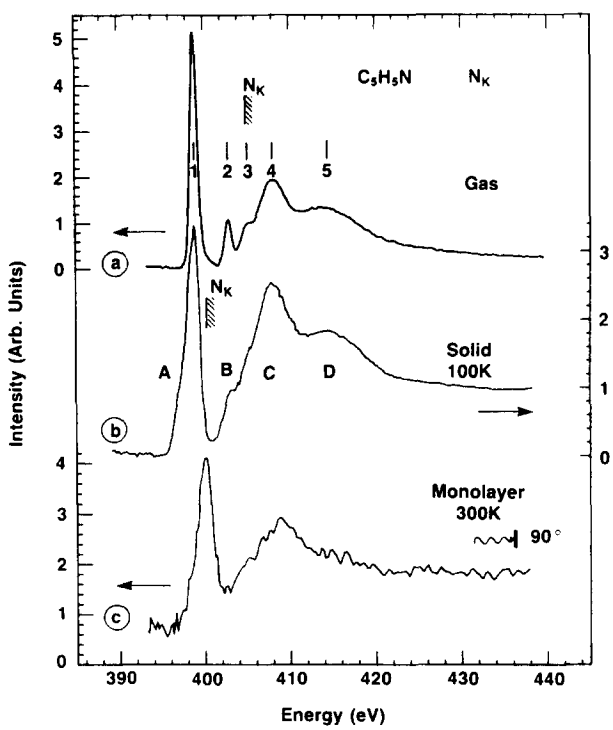

FIG. 4. (a) The nitrogen *K* shell ISEELS spectrum of gaseous pyridine recorded by 2.9 keV electron energy loss with 1.0 eV FWHM resolution. (b) The nitrogen *K* shell NEXAFS spectrum of solid (multilayer) pyridine at 100 K. (c) The nitrogen *K* shell NEXAFS spectrum of monolayer pyridine on Pt(111) recorded at 300 K with normal incidence.

The positions of the observed features at the N *K* edge are summarized in Table III. For the monolayer spectrum the $1s \rightarrow \pi^*$ resonance is shifted to higher energy by 1.3 eV, relative to the corresponding solid phase resonance.

IV. MULTIPLE SCATTERING CALCULATIONS

There are a number of conflicting assignments of the *K* shell resonances for benzene, in the literature. In earlier work,[8] peak A was assigned as a $1s \rightarrow \pi^*$ transition and peak B and the weaker peak between A and B were assigned to transitions to Rydberg states. The continuum peak C was assigned to a shake-up (two-electron excitation) transition. Benzene has two empty π^* orbitals, which should give rise to two resonances. Butscher *et al.*[15] have assigned peaks A and C to the two $1s \rightarrow \pi^*$ transitions, based on SCF-MO calculations, while Lindholm[16] has chosen peaks A and B, based on semiempirical HAM/3 calculations. Giordan *et al.*[17] have also suggested that peak B can be assigned to a transition to the second π^* state. The continuum peak D has been assigned to a σ^* shape resonance,[3] similar to the σ^* shape resonances observed in the spectra of simpler hydrocarbons.

The conflicting assignments as to the origin of transitions A, B, and C and the desire for a better understanding of continuum shape resonances in complex molecules in general, have led us to carry out multiple scattering (MS) $X\alpha$ calculations of the x-ray absorption cross sections for the carbon *K* edge of benzene. Because of the similar geometric and electronic structure of pyridine such calculations should also be able to help in the interpretation of the *K* shell spectra of this molecule.

The method of calculation followed the approach of Dehmer and Dill[18] in their calculation of the cross sections for the bound and continuum states at the *K* edge of N_2. The benzene potential was obtained from a self-consistent field calculation using the multiple scattering $X\alpha$ method.[19] The effect of the core hole was taken into account by using the transition state potential in which half an electron is removed from the 1*s* core orbital on one of the carbon atoms. Localized-hole broken-symmetry calculations provide the

Downloaded 18 Jun 2002 to 130.113.69.66. Redistribution subject to AIP license or copyright, see http://ojps.aip.org/jcpo/jcpcr.jsp

TABLE III. Absolute energies (eV) and assignments of features in the nitrogen *K* shell spectra of pyridine in the gas, solid, and monolayer states.

Feature	Gas ± 0.1 eV	Solid	Monolayer on Pt(111) 90°	Assignment
1 (A)	398.8[a]	398.8[b]	400.1[c]	π^*
2 (B)	402.7	403.3		π^*
3	405.1			continuum onset
4 (C)	408.0	408.0	408.2	σ^*
5 (D)	414.3	414.3		σ^*
I.P.	404.9[d]	400.2[e]		

[a] This feature was found to occur at 2.3(1) eV lower energy than the N $1s \rightarrow \pi^*$ feature in N_2 [401.1 eV (Ref. 39)].
[b] The original spectrum was shifted 1.4 eV to lower energy in order to align the first π^* peak with that of the gas phase spectrum.
[c] The recorded spectrum was shifted 1.4 eV to lower energy. The shift of 1.3 eV between solid and monolayer N $1s \rightarrow \pi^*$ is considered real.
[d] From gas phase XPS (Ref. 38).
[e] From solid state XPS (Ref. 37).

best description of the removal of an electron from a core orbital in a molecule containing equivalent atoms.[20,21] The benzene molecule symmetry was therefore reduced to C_{2v} in these calculations. The sphere radii and values of α were very close to one of the sets (set III) used by Case *et al.* in their series of MS-$X\alpha$ calculations on the benzene molecule.[22] They found that this set gave good agreement between calculated and experimental ionization potentials for the valence orbitals of benzene.

Oscillator strengths for the bound state transitions were calculated in the acceleration form of the dipole operator using the method of Noodleman.[23] The oscillator strengths were converted to cross sections following Dehmer and Dill,[18] using the relation

$$\sigma(E) = (\pi e^2 h/mc) df/dE = (\pi e^2 h/mc) f dn/dE,$$

where f is the oscillator strength and n is the principal quantum number. The height of the resonance is given by $\sigma(E)$ and the width by $(dn/dE)^{-1}$. The latter quantity is difficult to estimate for valence levels so, again following Dehmer and Dill,[18] we take the minimum experimentally observed gas phase width of 1 eV[8] as the width of the bound state resonance. Absorption cross sections for transitions from the core level to continuum states were calculated using the program of Davenport,[24] again with the acceleration form of the dipole operator.

The calculated continuum resonances were narrow (< 1 eV) and fairly intense, in contrast to the much broader features observed in the experimental spectrum. In addition to the broadening due to the instrumental resolution of 1 eV, there could be a substantial broadening due to the vibrational motion of the molecule, as demonstrated by Dehmer *et al.*[25] for N_2. A first principles calculation of this broadening would require a substantial computational effort, so in order to simulate the near edge region for comparison with experiment the continuum cross section was convoluted with a Lorentzian function of FWHM 3 eV, which is the approximate width of the first continuum resonance in the gas phase spectrum.

The calculated near edge spectrum obtained by combining the bound state and continuum calculations is shown in Fig. 5 together with the experimental gas phase spectrum for comparison. The agreement with the experimental spectra for gas phase and solid benzene is quite good and the positions and relative heights of the four principal peaks are well reproduced by the calculation. There are, however, five calculated resonances, with peak D corresponding to transitions to two closely spaced σ^* continuum resonances.

The assignment of the first two resonances, A and B, is straightforward. They correspond to transitions to the unoccupied e_{2u} and b_{2g} π^* orbitals. The weak feature (2) between these two peaks is assigned to a transition to a 3*p* Rydberg orbital. The assignment of the continuum resonances is less clear, however, as there are a larger number of σ^* states that can be obtained from the combination of the in-plane carbon orbitals. According to the correlation diagram for benzene

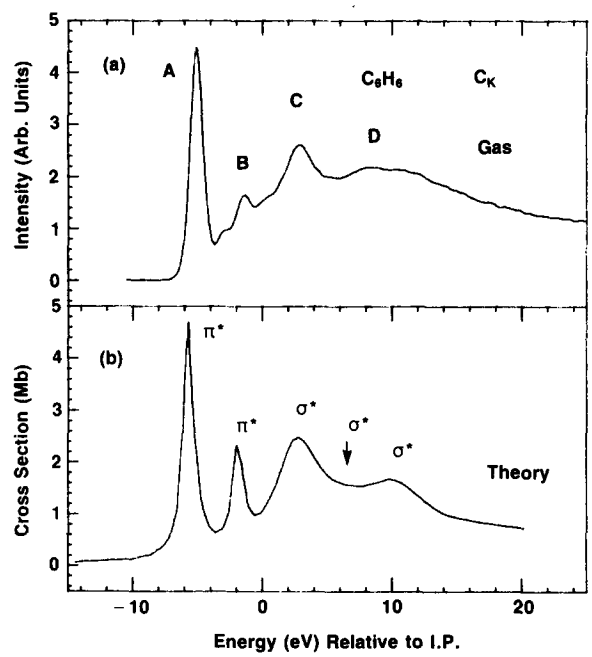

FIG. 5. Comparison of the experimental and calculated gas phase carbon *K* edge spectra of benzene. The calculated spectrum has been shifted so that the ionization threshold matches that determined experimentally by XPS.

Downloaded 18 Jun 2002 to 130.113.69.66. Redistribution subject to AIP license or copyright, see http://ojps.aip.org/jcpo/jcpcr.jsp

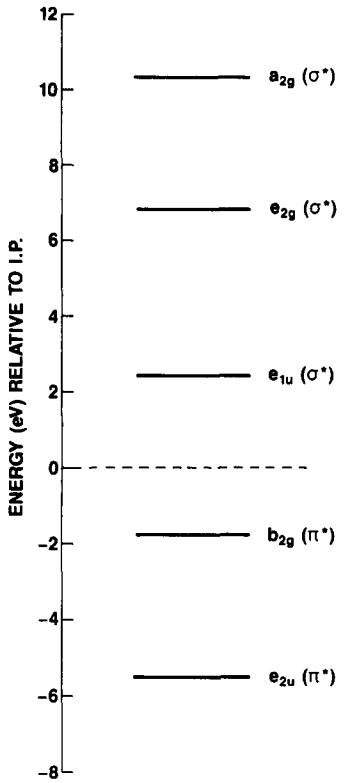

FIG. 6. Energy level diagram of calculated *K* edge excitations in benzene. The calculated relative energies of the upper states of the resonances are shown.

given by Herzberg,[26] the lowest-lying orbitals are, in order to increasing energy, of e_{2g}, a_{1g}, and a_{2g} symmetry, with b_{1u} and e_{1u} orbitals at a somewhat higher energy from this group. A partial assignment of the resonances can be made on the basis of their calculated polarization dependence in the broken symmetry calculation. For the excited carbon atom we define local x and y axes in the plane of the molecule, with the x axis pointing towards the center of the ring. The calculation shows that the first two continuum resonances are obtained if the E vector is parallel to either the x or y axis. However, the third resonance is obtained only for radiation with the E vector parallel to the y axis. Therefore, on the basis of the correlation diagram, the first two continuum resonances are assigned to continuum states of either e_{2g} or e_{1u} symmetry, obtained mainly from a combination of the $2p_x$ and $2p_y$ orbitals on each carbon atom, and the third resonance is assigned to a transition to a continuum state of a_{2g} symmetry obtained mainly from a combination of the $2p_y$ orbitals on the carbon atoms. Transitions to states of a_{1g} and b_{1u} symmetry, which would be observed when the E vector is parallel to the x axis, are evidently very weak.

For the first two continuum resonances it remains to be determined whether the continuum state has e_{2g} or e_{1u} symmetry. Herzberg[26] places the e_{1u} state higher in energy than both the e_{2g} and a_{2g} states. However, we have carried out an *ab initio* SCF-MO calculation on the benzene molecule with a minimal (STO-3G) basis set which placed the $e_{1u}\sigma^*$ virtual orbital below the e_{2g} and $a_{2g}\sigma^*$ virtual orbitals. Kreile *et al.*[27] have found that there is a good correlation between shape resonance position and the position of the corresponding virtual orbital obtained in a minimal basis set SCF-MO calculation on the neutral molecule. Further, a calculation of the continuum cross sections using the ground state potential with the full D_{6h} symmetry gave a strong resonance for transitions to e_{1u} continuum states and a weak resonance, at a higher energy, for transitions to e_{2g} continuum states. We therefore assign the first continuum resonance to a state of e_{1u} symmetry and the second to a state of e_{2g} symmetry. The calculated transitions at the carbon *K* edge in benzene are shown in an energy level diagram in Fig. 6, and the calculated energies and intensities for all the resonances are summarized in Table IV.

The width and intensity of continuum resonances are governed by the height of the effective potential barrier to escape of the photoelectron. Effective potential barriers can arise from centrifugal barriers in high angular momentum states of the escaping electron. The sharpness and intensity of the calculated continuum resonances in benzene indicate a high potential barrier. Following the method of Dehmer and Dill[18] and Davenport[24] the cross section was calculated as the sum of terms, each corresponding to a given l and m partial wave component of the wave function of the escaping photoelectron. Inspection of the different l components of this sum show that for the second (e_{2g}) and third (a_{2g}) continuum resonances the asymptotic wave function for the continuum state has predominantly $l = 6$ character. The first continuum resonance (e_{1u}) has predominantly $l = 5$ character, although there are substantial contributions from partial waves of lower angular momentum. The high angular momentum will produce a high centrifugal barrier, which

TABLE IV. Calculated relative energies and intensities of C *K* edge resonances in benzene.[a]

Upper state symmetry[b]	Energy relative to I.P. (eV)	Relative intensity (arb. units)	Predominant angular momentum state
$e_{2u}(\pi^*)$	− 5.5	1.0	...
$b_{2g}(\pi^*)$	− 1.77	0.43	...
$e_{1u}(\sigma^*)$	2.44	1.54	$l = 5$
$e_{2g}(\sigma^*)$	6.8	0.05	$l = 6$
$a_{2g}(\sigma^*)$	10.33	0.35	$l = 6$

[a] Parameters of MS-$X\alpha$ calculation: $\alpha_c = 0.759\,28$, $\alpha_H = 0.777\,25$, $\alpha_{INT} = 0.76$, $r_C = 1.6$ a.u., $r_H = 0.8$ a.u., $r_{OUT} = 5.486$ a.u., C–C distance = 2.636 a.u., C–H distance = 2.05 a.u.

[b] Calculations were carried out in C_{2v} symmetry; assignment corresponds to D_{6h} states from which the calculated states are derived.

Downloaded 18 Jun 2002 to 130.113.69.66. Redistribution subject to AIP license or copyright, see http://ojps.aip.org/jcpo/jcpcr.jsp

would explain the sharp calculated resonances. Addition of $l = 7$ and $l = 8$ outer sphere partial waves changed the cross section by less than 10^{-2} Mb.

The carbon $l = 2$ partial waves were found to have an important effect on the position and intensity of the σ^* continuum resonances. Without the $l = 2$ partial waves on the carbon atoms the resonances are still obtained but are shifted about 4 eV higher in energy than the continuum resonances shown in Fig. 5(b), and the relative intensities are also in poor agreement with experiment. In contrast, inclusion of the carbon $l = 2$ partial waves has a negligible effect on the positions and intensities of the π^* resonances.

Although MS $X\alpha$ calculations were not carried out for pyridine, the similarity of the benzene (Fig. 1) and pyridine (Figs. 2–4) spectra in the gas and solid states along with the isoelectronic nature of the two molecules strongly suggests that a generally similar set of states are involved in *K* shell excitation of pyridine. Thus we assign features A and B in both the carbon and nitrogen *K* edge spectra to π^* resonances while features C and D are attributed to σ^* resonances. As in gaseous benzene a weak feature (2) is observed as a shoulder between resonances A and B in the carbon *K* shell spectrum of gaseous pyridine [Fig. 3(a)]. This feature is absent from the spectrum of solid pyridine [Fig. 3(b)] confirming that it is a transition to a Rydberg state, probably the $3p$ state based on its term value of 3.2 eV.[28]

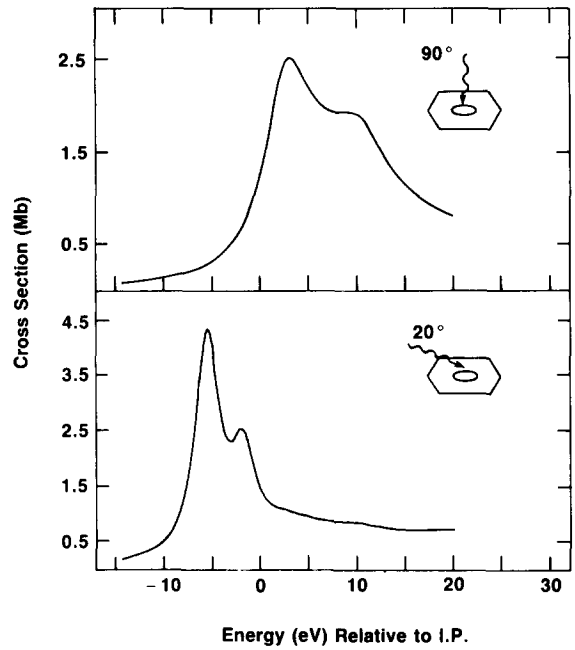

FIG. 7. The calculated carbon $1s$ spectrum of benzene for photoabsorption of linearly polarized light incident at (a) 90° and (b) 20° to the plane of the ring.

V. DISCUSSION

Our assignments of peaks A, B to π^* states and peaks C, D to σ^* states are strongly supported by the polarization dependence of the chemisorbed monolayer spectra shown in Figs. 1–4. In both benzene and pyridine peaks A and B have the opposite polarization dependence to peaks C and D, which indicates opposite symmetry of the first and second pairs of states. Figure 7 gives the calculated benzene *K* edge spectra for linearly polarized light incident at 90° and 20° with respect to the plane of the ring. Comparison of the two calculated spectra in Fig. 7 to those for chemisorbed benzene in Fig. 1 readily establishes that benzene lies down on the surface. In contrast, pyridine must be oriented perpendicular to the surface because of the opposite polarization dependence of the resonances.[7]

A parallel orientation to the surface for benzene and a perpendicular one for pyridine has been inferred before from the polarization dependence of peak A alone,[7] which clearly must correspond to a $1s \rightarrow \pi^*$ excitation. The persistence of peak B in the spectrum of the field is characteristic of valence states rather than Rydberg states, which are normally quenched in the solid state.[28] This result, together with the results of the calculation, unambiguously establishes peak B to be the second weaker $1s \rightarrow \pi^*(b_{2g})$ resonance. For chemisorbed benzene this resonance is not resolved but is part of the broad peak around 286 eV (Fig. 1). The existence of a second π^* resonance for chemisorbed benzene is furthermore supported by the comparison of NEXAFS spectra for ethylene, benzene, and pyridine monolayers chemisorbed on Pt(111) shown in Fig. 8. For all molecules we have indicated the chemisorption geometries. Although the C–C bonds for both ethylene and benzene are parallel to the surface the width of the first resonance, which corresponds to a $1s \rightarrow \pi^*$ excitation, is significantly broader for benzene.

Comparison of the spectra for chemisorbed benzene with those of chemisorbed pyridine (Fig. 8) clearly shows the effect of the interaction of the molecular π system with the surface. The hybridization of molecular π^* orbitals with metal orbitals (predominantly of *d* charcter) leads to a broadening of the π^* resonance but the broadening is much greater for benzene than for pyridine, since the plane of the pyridine ring is perpendicular to the surface. The origin of the broadening can be attributed to an energy broadening of the hybridized π^* state relative to the pure molecular π^* state (initial state effect) and/or to a reduced lifetime of the $1s \rightarrow \pi^*$ final state created in the x-ray absorption process. A reduced lifetime would result from the overlap of metal and molecular states as a consequence of delocalization. A similar broadening effect has been noted in the carbon and oxygen $1s \rightarrow \pi^*$ transitions of monolayer CO on Ni(111) and Pt(111).[29] This was attributed to broadening of the π^* level by hybridization with the $4s,4p$ states of the Ni substrates.

Although the absolute energies of the N *K* edge features in the solid and monolayer pyridine spectra could be in error by as much as 1 eV, the position of the $1s \rightarrow \pi^*$ resonance in the monolayer spectrum relative to the position of the corresponding resonance in the solid phase spectrum is known to an accuracy of about $\pm$ 0.5 eV. We consider, therefore, that the observed shift of 1.3 eV in the $1s \rightarrow \pi^*$ resonance at the N *K* edge of monolayer pyridine, relative to the solid phase position, is real. The shift could be caused either by a shift in the N $1s$ core level on chemisorption or by an antibonding interaction of the N $2p$ π orbital with the adjacent metal *d* orbitals. A shift of 1.4 eV to higher energy relative to gas phase pyridine has been observed in the N $1s$ core level in the $Fe(CO)_4$–pyridine complex.[30] The fact that the correspond-

Downloaded 18 Jun 2002 to 130.113.69.66. Redistribution subject to AIP license or copyright, see http://ojps.aip.org/jcpo/jcpcr.jsp

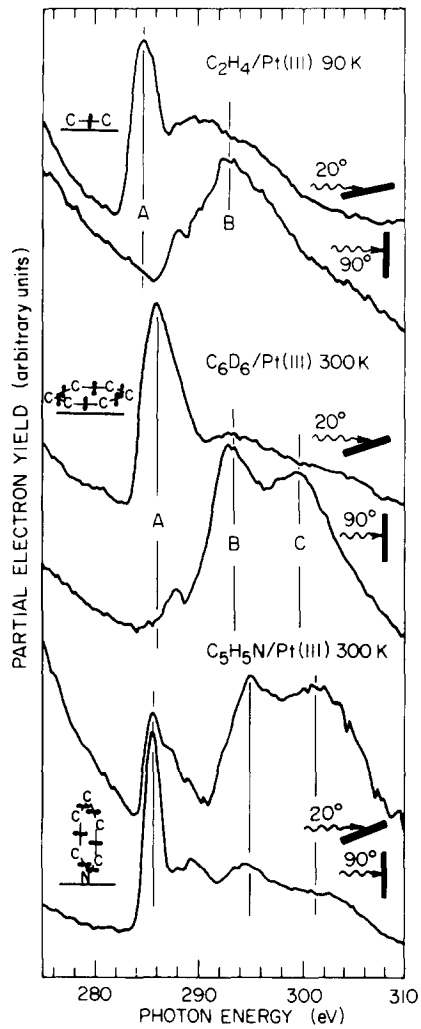

FIG. 8. The carbon *K* edge NEXAFS spectra of (a) C_2H_4, (b) C_6D_6, and (c) C_5H_5N monolayers on Pt(111). Spectra recorded with 90° and 20° incident radiation are shown for each species. The indicated orientation of each molecule to the surface is consistent with the polarization dependence of both the π^* and σ^* resonance intensities.

ing C *K* $1s \rightarrow \pi^*$ resonance in monolayer pyridine shows a shift of less than 0.5 eV is evidence that pyridine bonds to the Pt(111) surface through the nitrogen.

We have shown in previous work[2,3,5,6] that in most cases a given σ^* shape resonance can be associated with one of the bonds, or types of bond, in a molecule, and that the energy of the shape resonance (relative to E_v for gas phase molecules and relative to E_F for chemisorbed molecules) is a sensitive measure of the bond length. For example, we have shown that for aliphatic hydrocarbons there is a σ^* shape resonance corresponding to each type of carbon–carbon bond in the molecule and that there is a linear relationship between the σ^* shape resonance position, relative to E_v or E_F, and the length of the corresponding bond.[2,3] If these results could be extended to aromatic molecules we would expect to find only one σ^* shape resonance in the benzene spectrum, corresponding to the unique C–C bond length. However, for benzene there are two distinctly resolved and three calculated shape resonances. The difference between the aliphatic and aromatic hydrocarbons can be understood by building up the correct delocalized σ^* states from a set of localized σ^* states,[31] each of these being localized on one of the bonds in the molecule. In the case of the aliphatic molecules there is only a weak interaction between the localized σ^* states[31] and so the delocalized σ^* states corresponding to a given type of bond all lie at about the same energy, producing only one shape resonance. However, in benzene and other aromatic molecules there is a strong interaction between the localized σ^* states, producing a set of delocalized σ^* states that are widely separated in energy. In our previous work,[2,3] we used only peak D in the correlation of bond length with shape resonance position, which is incorrect in the light of our present results. We note, however, that for benzene the intensity weighted *average* energy of peaks C and D relative to E_v, 8.8 ± 0.5 eV, is in good agreement with the predicted value[3] of 8.5 ± 0.5 eV for a bond length of 1.40 Å with a single associated shape resonance.

In pyridine the average C–C bond length (1.394 Å) is about 0.05 Å longer than the C–N bond length (1.340 Å).[32] The simple correlation[2,3] for $Z = 12$ (C–C) and 13 (C–N) predicts that the average σ shape resonance energy associated with these bond lengths will occur at 8.8 (5) eV above the C *K* I.P. and at 5.2(5) eV above the N *K* I.P. Experimentally, the intensity weighted average energy relative to the I.P. is 8.7 (5) eV for the C *K* edge spectrum and 6.0 (5) eV in the N *K* edge spectrum. Both the C–C bond length and the C–N bond length are therefore obtained within 0.02 Å of experiment using the simple correlation. The shift in the intensity weighted average energy shows up experimentally as a change in the relative intensities of the continuum peaks. The intensity of peak C relative to peak D is greater at the N *K* edge than at the C *K* edge.

Despite the complexity of the spectra, changes in the bond length on formation of the solid and on chemisorption should be reflected by changes in the σ^* shape resonance position. Comparison of the spectra for gas phase, solid, and chemisorbed benzene and pyridine shows that both σ^* peaks move by at most 1 eV. This corresponds to a maximum bond length change of 0.02 Å, using the relationship established previously.[3] The bond length in solid benzene is indeed known to be almost identical to the gas phase value.[33] There are no reported measurements of the bond length in chemisorbed benzene on Pt(111). From low energy electron diffraction studies, Van Hove *et al.*[34] suggested that in the case of benzene chemisorbed on Rh(111) the benzene ring is distorted to lower (C_{3v}) symmetry with alternating C–C bond lengths of 1.6 ± 0.1 and 1.25 ± 0.1 Å. Our results clearly indicate that there is no distortion of this magnitude for benzene on Pt(111), as such large changes in bond length would lead to substantial changes in the shape resonance positions on chemisorption. Our conclusion that there is a change of at most 0.02 Å in the C–C bond length on chemisorption is consistent with x-ray diffraction measurements of the C–C bond length in organometallic π complexes of benzene, where the observed change in bond length is also less than 0.02 Å.[35,36]

VI. CONCLUSIONS

Comparison of the *K* shell spectra for gas phase, solid state, and chemisorbed benzene and pyridine, together with

Downloaded 18 Jun 2002 to 130.113.69.66. Redistribution subject to AIP license or copyright, see http://ojps.aip.org/jcpo/jcpcr.jsp

a multiple scattering $X\alpha$ calculation of the benzene K shell cross sections, has enabled us to assign all the principal features in the spectra. Carbon and nitrogen K shell spectra of gas phase pyridine are reported for the first time. For benzene, in addition to the two expected π^* resonances, calculations indicate that there are three σ^* resonances (two of which merge to form one peak in the experimental spectrum), corresponding to high ($l = 5$ and 6) angular momentum states of the escaping photoelectron. There is at most only a 1 eV change in the positions of the σ^* resonances on formation of the solid and chemisorbed phases in these molecules, which leads us to conclude that the maximum change in the carbon–carbon bond length is only 0.02 Å. This is in agreement with earlier x-ray diffraction measurements on solid benzene and is consistent with x-ray diffraction measurements of the bond length in organometallic π complexes of benzene. Finally, the polarization dependence of both the π^* and σ^* resonances in the monolayer spectra has shown that benzene lies flat on Pt(111) while the plane of the pyridine molecule at 300 K is perpendicular to the surface.

ACKNOWLEDGMENTS

The work carried out at McMaster University was supported by NSERC (Canada). A. P. Hitchcock acknowledges personal support through an NSERC University Research Fellowship. Portions of the work reported here were done at SSRL which is supported by the Office of Basic Energy Sciences at DOE and the Division of Materials Research of NSF.

[1]C. E. Brion, S. Daviel, R. N. S. Sodhi, and A. P. Hitchcock, AIP Conf. Proc. **94**, 426 (1982); A. P. Hitchcock, J. Electron Spectrosc. Relat. Phenom. **25**, 245 (1982).
[2]A. P. Hitchcock, S. Beaulieu, T. Steel, J. Stöhr, and F. Sette, J. Chem. Phys. **80**, 3927 (1984).
[3]F. Sette, J. Stöhr, and A. P. Hitchcock, J. Chem. Phys. **81**, 4906 (1984).
[4]J. Stöhr, in *Chemistry and Physics of Solid Surfaces V*, edited by R. Vanselow and R. Howe (Springer, Berlin, 1984), p. 231.
[5]J. Stöhr, J. L. Gland, W. Eberhardt, D. Outka, R. J. Madix, F. Sette, R. J. Koestner, and U. Doebler, Phys. Rev. Lett. **51**, 2414 (1983).
[6]J. Stöhr, F. Sette, and A. L. Johnson, Phys. Rev. Lett. **53**, 1684 (1984).
[7]A. L. Johnson, E. L. Muetterties, and J. Stöhr, J. Am. Chem. Soc. **105**, 7183 (1983).
[8]A. P. Hitchcock and C. E. Brion, J. Electron Spectrosc. Relat. Phenom. **10**, 317 (1977).
[9]S. Lehwald, H. Ibach, and J. E. Demuth, Surf. Sci. **78**, 577 (1978).
[10]F. P. Netzer and J. A. D. Matthew, Solid State Commun. **29**, 209 (1979).
[11]J. C. Bertolini and J. Rousseau, Surf. Sci. **89**, 467 (1979).
[12]D. W. Davis and D. A. Shirley, J. Electron Spectrosc. Relat. Phenom. **3**, 157 (1974).
[13]D. T. Clark and D. Kilcast, J. Chem. Soc. B **1971**, 2243.
[14]J. Stöhr and R. Jaeger, Phys. Rev. B **26**, 4111 (1982).
[15]W. Butscher, W. H. E. Schwarz, and K. H. Thunemann, in *Inner-Shell and X-Ray Physics of Atoms and Solids*, edited by D. J. Fabian, H. Kleinpoppen, and L. Watson (Plenum, New York, 1981).
[16]E. Lindholm, J. Chem. Phys. (in press).
[17]J. C. Giordan, J. H. Moore, and J. A. Tossel, J. Am. Chem. Soc. (in press).
[18]J. L. Dehmer and D. Dill, J. Chem. Phys. **65**, 5327 (1976).
[19]J. C. Slater and K. H. Johnson, Phys. Rev. B **5**, 844 (1972).
[20]P. S. Bagus and H. F. Schaeffer III, J. Chem. Phys. **56**, 224 (1972).
[21]G. Loubriel, Phys. Rev. B **20**, 5339 (1979).
[22]D. A. Case, M. Cook, and M. Karplus, J. Chem. Phys. **73**, 3294 (1980).
[23]L. Noodleman, J. Chem. Phys. **64**, 2343 (1976).
[24]J. W. Davenport, Phys. Rev. Lett. **36**, 945 (1976).
[25]J. L. Dehmer, D. Dill, and A. C. Parr, in *Photophysics and Photochemistry in the Vacuum Ultraviolet*, edited by S. P. McGlynn, G. Findley, and R. Huebner (Reidel, Dordrecht, Holland, 1983).
[26]G. Herzberg, *Electronic Spectra of Polyatomic Molecules* (Van Nostrand, New York, 1960), p. 398.
[27]J. Kreile, A. Schweig, and W. Thiel, Chem. Phys. Lett. **108**, 259 (1984).
[28]M. B. Robin, *Higher Excited States of Polyatomic Molecules* (Academic, New York, 1974), Vol. 1.
[29]Y. Jugnet, F. J. Himpsel, Ph. Avouris, and E. E. Koch, Phys. Rev. Lett. **53**, 198 (1984); F. Sette, J. Stöhr, E. B. Kollin, D. J. Dwyer, J. L. Gland, J. L. Robbins, and A. L. Johnson, *ibid.* **54**, 935 (1985).
[30]D. B. Beach, S. P. Smit, and W. L. Jolly, Organometallics **3**, 556 (1984).
[31]W. L. Jorgensen and L. Salem, *The Organic Chemists Book of Orbitals* (Academic, New York, 1973).
[32]*Tables of Interatomic Distances*, Special Publ. No. 11 (The Chemical Society, London, 1958).
[33]E. G. Cox, Rev. Mod. Phys. **30**, 159 (1958).
[34]M. A. Van Hove, R. F. Lin, and G. A. Somorjai, Phys. Rev. Lett. **51**, 778 (1983).
[35]E. Keulen and F. Jellinek, J. Organomet. Chem. **5**, 490 (1966).
[36]B. Rees and P. Coppens, Acta Crystallogr. Sect. B **29**, 2516 (1973).
[37]D. J. Clark, R. D. Chamber, D. Kilcast, and W. K. R. Musgrave, J. Chem. Soc. Faraday Trans. 2 **68**, 309 (1972).
[38]A. A. Bakke, H. W. Chen, and W. L. Jolly, J. Electron Spectrosc. Relat. Phenom. **20**, 333 (1980).
[39]R. N. S. Sodhi and C. E. Brion, J. Electron Spectrosc. Relat. Phenom. **34**, 363 (1984).

Downloaded 18 Jun 2002 to 130.113.69.66. Redistribution subject to AIP license or copyright, see http://ojps.aip.org/jcpo/jcpcr.jsp